

Catalysis Science & Technology

Accepted Manuscript



This article can be cited before page numbers have been issued, to do this please use: B. Han, L. Zhao, Y. Song, Z. Zhao, D. Yang, R. Liu and G. Liu, *Catal. Sci. Technol.*, 2018, DOI: 10.1039/C8CY00648B.



This is an Accepted Manuscript, which has been through the Royal Society of Chemistry peer review process and has been accepted for publication.

Accepted Manuscripts are published online shortly after acceptance, before technical editing, formatting and proof reading. Using this free service, authors can make their results available to the community, in citable form, before we publish the edited article. We will replace this Accepted Manuscript with the edited and formatted Advance Article as soon as it is available.

You can find more information about Accepted Manuscripts in the [author guidelines](#).

Please note that technical editing may introduce minor changes to the text and/or graphics, which may alter content. The journal's standard [Terms & Conditions](#) and the ethical guidelines, outlined in our [author and reviewer resource centre](#), still apply. In no event shall the Royal Society of Chemistry be held responsible for any errors or omissions in this Accepted Manuscript or any consequences arising from the use of any information it contains.

A super-hydrophobic mesostructured silica as a chiral organometallic immobilization platform for heterogeneous asymmetric catalysis

Bing Han, Lei Zhao, Yongkang Song, Zhongrui Zhao, Dongfeng Yang, Rui Liu,* Guohua Liu*

Received (in XXX, XXX) Xth XXXXXXXXX 200X, Accepted Xth XXXXXXXXX 200X

5 First published on the web Xth XXXXXXXXX 200X

DOI: 10.1039/b000000x

Immobilization of molecule catalysts in a super-hydrophobic material can efficiently overcome the shortage of low catalytic efficiency in heterogeneous catalysis. In this work, by taking advantage of a super-hydrophobic mesostructured silica as a support, we incorporate conveniently chiral diamine within its silicate network, constructing two hydrophobic rhodium/diamine- and ruthenium/diamine-functionalized heterogeneous catalysts. Analyses *via* solid-state carbon spectra disclose the well-defined single-site active species in their silicate framework, and that with water contact angle measurements reflects their highly hydrophobicity nature. Characterizations *via* scanning and transmission electron microscopy reveal their monodispersed feature. As presented in the study, the hydrophobic rhodium/diamine-functionalized catalyst promotes greatly the enantioselective tandem reduction/lactonization of ethyl 2-acylarylcarboxylates to give various chiral phthalides, whereas the hydrophobic ruthenium/diamine-functionalized catalyst boosts an efficient asymmetric transfer hydrogenation-dynamic kinetic resolution process for construction of 1,2-distereocentered diethyl α -benzoyl- β -hydroxyphosphonates. As we envisaged, the as-made catalysts with high hydrophobicity and uniformly distributed single-site catalytically active nature make combinational contributions in their catalytic performances, affording chiral products in high yields with up to 99% enantioselectivity. Moreover, catalyst can be also recovered easily and recycled repeatedly, making it an attracting feature in an efficiently organic transformation.

1. Introduction

25 Development of mesostructured silicas as supports to immobilize chiral organometallic complexes for heterogeneous asymmetric catalysis has made great achievement recently.¹ Especially, some prominent properties of mesostructured silica, such as confinement effect and synergistic effect, have produced many superior heterogeneous catalysts to their homogeneous ones, which complement nicely the drawbacks of heterogeneous catalysis.² Therefore, utilization of functional mesoporous silica as a support fabricating highly efficient heterogeneous catalysts represents an attracting research direction in heterogeneous asymmetric catalysis.

35 Super-hydrophobic mesostructured silicas³ possess the feature of super-hydrophobic materials⁴ and advantage of inorganosilicate nanoparticles.⁵ Combining both benefits in the construction of the super-hydrophobic mesostructured silica-supported molecule catalysts has great superiority in heterogeneous asymmetric catalysis.⁶ For the hydrophobic benefit, heterogeneous catalysts enable a highly efficient mass transfer in support, which can greatly overcome the disadvantage of slow reaction rate in a general heterogeneous catalysis. Furthermore, super-hydrophobic feature also ensures a high dispersion in organic reaction system, which can result in a homo-like catalytic environment and enhance

catalytic efficiency. Moreover, in some special cases, for example, in the case of reaction with water-soluble products, the super-strong water repellent ability guarantees a timely desorption of products, boosting greatly catalytic performance.⁶ For the mesostructured silica-support benefit, large surface area and pore volume, tunable pore dimension and well-defined pore arrangement, and high thermal and mechanical stabilities not only allow an efficient immobilization of chiral organometallic complexes for a maintainable catalytic performance but also realize a reliable recycling *via* simple nanofiltration. Despite some scattered reports made in construction of super-hydrophobic mesoporous silicas for catalysis,³ exploration of their applications in an enantioselective reaction has not been explored yet. Thus, fabrication of a super-hydrophobic mesostructured silica-supported chiral molecule catalyst with enhanced catalytic activity and selectivity in an enantioselective reaction is a significant challenge in heterogeneous asymmetric catalysis.

As efforts aimed at exploration of heterogeneous catalysts for enantioselective reactions,⁷ in this contribution, we utilize a super-hydrophobic mesostructured silica as a support, and combine chiral diamine within its silicate network to establish a chiral diamine-modified mesostructured silica platform. It not only offers a practical approach to prepare two hydrophobic heterogeneous catalysts, but also performs two type of efficiently enantioselective reactions. As demonstrated in this study, the chiral rhodium/diamine-functionalized heterogeneous catalyst promotes greatly the enantioselective tandem reduction/lactonization of ethyl 2-acylarylcarboxylates to construct chiral phthalides, and the chiral ruthenium/diamine-functionalized heterogeneous catalyst

Key Laboratory of Resource Chemistry of Ministry of Education, Shanghai Key Laboratory of Rare Earth Functional Materials, Shanghai Normal University, Shanghai, 200234, China.

50 E-mail: rliu@shnu.edu.cn; ghliu@shnu.edu.cn, Fax: 86-21-64322511; Tel: 86-21-64322280.

enables a asymmetric transfer hydrogenation–dynamic kinetic resolution process for synthesis of various 1,2–distereocentered diethyl α –benzoyl– β –hydroxyphosphonates.

2. Experimental

2.1. Characterization

Ru and Rh loading amounts in this catalysts were analyzed using an inductively coupled plasma optical emission spectrometer (ICP–OES, Varian VISTA–MPX). Fourier transform infrared (FT–IR) spectra were collected on a Nicolet Magna 550 spectrometer using a KBr method. Scanning electron microscopy (SEM) image was obtained using a JEOL JSM–6380LV microscope operating at 20 kV. Transmission electron microscopy (TEM) image was performed on a JEOL JEM2010 electron microscope at an acceleration voltage of 220 kV. Nitrogen adsorption isotherms were measured at 77 K with a Quantachrome Nova 4000 analyzer. The samples were measured after being outgassed at 423 K overnight. Pore size distributions were calculated by using the BJH model. The specific surface areas (S_{BET}) of samples were determined from the linear parts of BET plots ($p/p_0 = 0.05$ – 1.00). Solid–state NMR experiments were explored on a Bruker AVANCE spectrometer at a magnetic field strength of 9.4 T with ^1H frequency of 400.1 MHz, ^{13}C frequency of 100.5 MHz and ^{29}Si frequency of 79.4 MHz with 4 mm rotor at two spinning frequency of 5.5 kHz and 8.0 kHz, TPPM decoupling is applied in the during acquisition period. ^1H cross polarization in all solid–state NMR experiments were employed using a contact time of 2 ms and the pulse lengths of 4 μs .

2.2. Catalyst 5 preparation

In a typical synthesis, (*The first step for the synthesis of 3*) 0.40 g (0.27 mmol) of cetyltrimethylammonium bromide (CTAB) was added to an aqueous solution (180 mL) of NaOH (1.40 mL, 2 M) at 70 °C. After dissolution of CTAB, 1.136 mL (0.50 mmol) of mesitylene (TMB) was added to the system. The mixture was sonicated for one hour to form stable white emulsion. tetraethoxysilane (TOES) (2.00 mL, 9.0 mmol) and ethyl acetate (1.60 mL) was then added, and the mixture was stirred for 10 minute. After that, 0.50 g (1.0 mmol) of (*S,S*)–4–(trimethoxysilyl)ethylphenylsulfonyl–1,2–diphenylethylenediamine (**1**) was added dropwise to the system, the mixture was stirred for another 10 minute. Finally, 2.10 mL (10.0 mmol) of diphenyldichlorosilane (**2**) was added to the system. After being stirred for another two hours at 70 °C, the mixture was transferred to the autoclaves and kept aging at 100 °C for 24 h. After cooling to room temperature, the solids were collected by centrifugation and washed repeatedly with excess distilled water. The surfactant template was removed by refluxing in a solution (160.0 mg of ammonium nitrate in 250 mL of ethanol) at 60 °C for 12 h. The solids was filtered and washed with excess water and ethanol, and dried at ambient temperature under vacuum overnight to afford Ph@ArDPEN@MSNs (**3**) as a white powder (1.86 g). (*The second step for the synthesis of 5*) The collected solids (0.50 g) was suspended in 20.0 mL of dry CH_2Cl_2 , 61.80 mg (0.10 mmol) of $(\text{Cp}^*\text{RhCl}_2)_2$ (**4**) was added and the resulting mixture was stirred at 25 °C for 12 h. The mixture was filtered through filter paper and then rinsed with excess CH_2Cl_2 . After Soxhlet extraction for 24 h

in CH_2Cl_2 to remove homogeneous and unreacted starting materials, the solid was dried at ambient temperature under vacuum overnight to afford Ph@Cp*RhArDPEN@MSNs (**5**) (0.52 g) light–yellow powder. ICP analysis showed that the Rh–loading was 9.516 mg (0.09239 mmol of Rh) per gram of catalyst. ^{13}C CP/MAS NMR (161.9 MHz): 154.9–125.5 (C of –SiPh₂, Ph and Ar groups), 96.1 (C of Cp ring), 69.2–58.3 (C of –NCHPh, and of –NCH₂– in CTAB molecule), 40.1–25.2 (C of –CH₂Ar, and of –CH₂– in CTAB molecule), 20.6–12.5 (C of CH₃– in CTAB molecule), 10.7 (C of –CH₃ in Cp(CH₃)₅), 2.2 (C of –CH₂Si) ppm. ^{29}Si MAS NMR (79.4 MHz): D¹ ($\delta = -40.2$ ppm), D² ($\delta = -47.9$ ppm), T² ($\delta = -61.4$ ppm), T³ ($\delta = -71.1$ ppm), Q² ($\delta = -94.9$ ppm), Q³ ($\delta = -105.1$), Q⁴ ($\delta = -113.4$) ppm.

2.3. Catalyst 8 preparation

Prepared according to the above general procedure **5** using (mesityleneRuCl₂)₂ (**7**) instead of (Cp*RhCl₂)₂ (**4**), the solid was dried under reduced pressure overnight to afford Ph@MesityleneRuArDPEN@MSNs (**8**) light–yellow powder. ICP analysis showed that the Ru–loading was 4.002 mg (0.03923 mmol of Ru) per gram of catalyst. ^{13}C CP/MAS NMR (161.9 MHz): 154.8–125.6 (C of –SiPh₂, Ph and Ar groups), 106.1, 102.3 (C of aromatic carbons in Mesitylene groups), 64.7–60.1 (C of –NCHPh, and of –NCH₂– in CTAB molecule), 39.3–23.5 (C of –CH₂Ar, and of –CH₂– in CTAB molecule), 20.8 (C of –CH₃ in Mesitylene(CH₃)₃), 14.6 (C of CH₃– in CTAB molecule), 1.5 (C of –CH₂Si) ppm. ^{29}Si MAS NMR (79.4 MHz): D¹ ($\delta = -38.5$ ppm), D¹ ($\delta = -43.9$ ppm), T² ($\delta = -60.1$ ppm), T³ ($\delta = -67.8$ ppm), Q² ($\delta = -93.6$ ppm), Q³ ($\delta = -101.3$ ppm), Q⁴ ($\delta = -110.5$) ppm.

2.4. General procedure for the asymmetric synthesis of chiral phthalides

A typical procedure was as follows. Catalyst **5** (21.65 mg, 2.0 μmol of Rh based on ICP analysis), HCO₂Na (1.0 mmol), 2–acylarylcarboxylates (0.20 mmol) and 3.0 mL of the mixed solvents (MeOH/H₂O, v/v = 2/1) were added in 5 mL flask purged with nitrogen in turn. The mixture was allowed to react at 40 °C for 5–10 h. During that time, the reaction was monitored constantly by TLC. After completion of the reaction, the heterogeneous catalyst was separated *via* centrifuge (10000 r/minute) for the recycle experiment. The aqueous solution was extracted by Et₂O (3 \times 3.0 mL). The combined Et₂O was washed with brine twice and dehydrated with Na₂SO₄. After the evaporation of Et₂O, the residue was purified by silica gel flash column chromatography to afford the desired products.

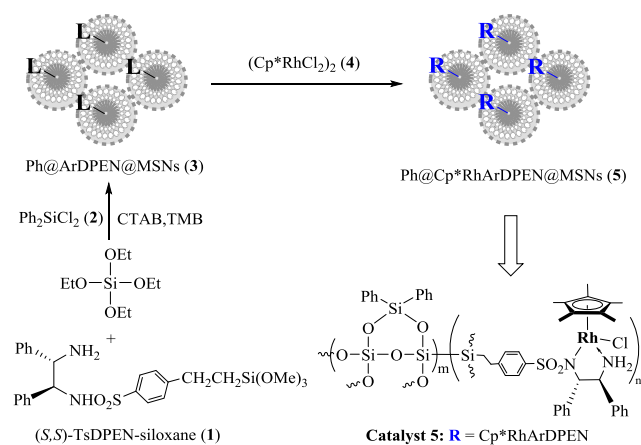
2.5. General procedure for the DKR–ATH of α –benzoyl– β –ketophosphonates

A typical procedure was as follows. Catalyst **8** (12.75 mg, 0.50 μmol of Ru based on ICP analysis), α –benzoyl– β –ketophosphonates (0.10 mmol), and 0.10 mL (20.0 mmol) of HCOOH–Et₃N (5:2), and 3.0 mL of CH_2Cl_2 were added sequentially to a 10.0 mL round–bottom flask. The mixture was then stirred at 35 °C for 24–30 h. During this period, the reaction was monitored constantly by TLC. After completion of the reaction, the catalyst was separated by centrifugation (10,000 rpm) for the recycling experiment. The aqueous solution was extracted with ethyl ether (3 \times 3.0 mL). The combined ethyl ether extracts

were washed with brine twice and then dehydrated with Na_2SO_4 . After evaporation of ethyl ether, the residue was purified by silica gel flash column chromatography to afford the desired products.

3. Results and discussion

3.1. Synthesis and structural characterization of the heterogeneous catalysts



Scheme 1. Preparation of heterogeneous catalyst 5.

Assembly of chiral catalytically active centers within the network of super-hydrophobic mesostructured silica to produce the rhodium/diamine-functionalized heterogeneous catalyst, abbreviated as $\text{Ph@Cp}^*\text{RhArDPEN@MSNs}$ (**5**) ($\text{Cp}^*\text{RhArDPEN}$:⁸ Cp^* = pentamethyl cyclopentadiene and ArDPEN = (*S,S*)-4-((trimethoxysilyl)ethyl)phenylsulfonfyl-1,2-diphenylethylene-diamine) could be performed *via* a simple two-step procedure as outlined in Scheme 1. In first step, three-component condensation of tetraethoxysilane (TOES), (*S,S*)-TsDPEN-siloxane (**1**) and Ph_2SiCl_2 (**2**) through the use of cetyltrimethylammonium bromide (CTAB) as a structure-directing template and mesitylene (TMB) as micelle swelling agent afforded the chiral ArDPEN-modified Ph@ArDPEN@MSNs (**3**) as a white powder. In second step, direct complexation of **3** with $(\text{Cp}^*\text{RhCl}_2)_2$ (**4**), followed by a purified Soxhlet extraction, provided the pure catalyst **5** as a light-yellow powder (see Fig. S1 of ESI).

Well-defined single-site chiral rhodium/diamine active center incorporated in its hydrophobic silicate network of **5** could be proven by its solid-state ^{13}C cross-polarization (CP)/magic angle spinning (MAS) NMR spectroscopy. As shown in Figure 1, the solid-state ^{13}C CP/MAS NMR spectra of **3** and catalyst **5** produced the strong carbon signals of phenyl groups in the $-\text{SiCPh}_2$ moiety around 136 ppm, which were correspond to the hydrophobic organosilica. In the part of chiral rhodium/diamine complex, besides the general carbon signals around 63 ppm and around 130 ppm for the carbon atoms of the $-\text{NCHPh}$ groups and of the $-\text{C}_6\text{H}_5$ groups in ArDPEN moiety, the characteristic peak at 96.1 ppm in the spectrum of **5** ascribed to the carbon atoms of the Cp^* rings while that at 10.7 ppm was attributed to the carbon atom of the CH_3 groups attached to the Cp^* ring. These characteristic peaks were absent in the spectrum of **3**, suggesting the formation

of the well-defined single-site $\text{Cp}^*\text{RhArDPEN}$ species because these chemical shifts are similar to those of its homogeneous $\text{Cp}^*\text{RhTsDPEN}$.⁹ These findings confirmed that immobilization of chiral $\text{Cp}^*\text{RhArDPEN}$ -functionality within its silicate network could keep the original chemical environment of the corresponding homogeneous $\text{Cp}^*\text{RhTsDPEN}$.

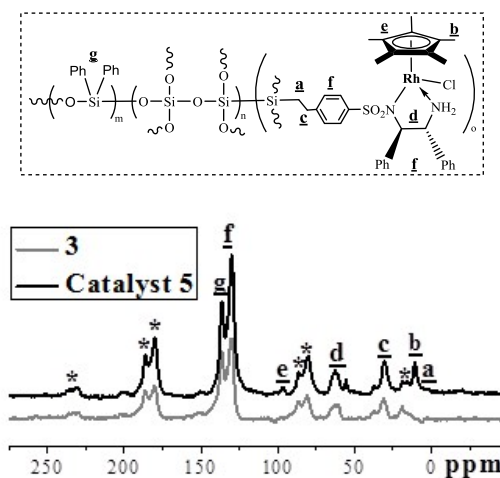


Fig. 1 Solid-state ^{13}C CP/MAS NMR spectra of **3** and catalyst **5**.

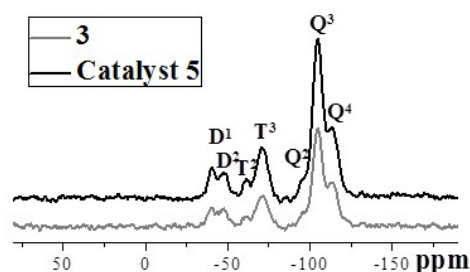


Fig. 2 Solid-state ^{29}Si MAS NMR spectra of **3** and catalyst **5**.

Figure 2 showed the solid-state ^{29}Si MAS NMR spectra **3** and catalyst **5**, which further demonstrated the compositions of their silicate networks. It was found that both **3** and catalyst **5** had three groups of typical signals (Q-, T- and D-series), where Q signals were attributed to inorganosilica, T signals were corresponding to $-\text{SiCH}_2-$ groups of organosilica, and D signals ascribed to hydrophobic $-\text{SiCPh}_2$ groups of organosilica, respectively. As compared these values of **5** with those typical ones in the literature,¹⁰ the strong Q^3 - Q^4 signals at -105.1 and -113.4 ppm demonstrated the $(\text{HO})\text{Si}(\text{OSi})_3$ and $\text{Si}(\text{OSi})_4$ species as its inorganosilicate wall, whereas the T^3 signal at -71.1 ppm indicated the $\text{R}-\text{Si}(\text{OSi})_3$ species (R = $\text{Cp}^*\text{RhTsDPEN}$ -linked alkyl-functionality) as its one part of organosilica. Characteristic D signals for D^1 and D^2 at -40.2 and -47.9 ppm confirmed that super-hydrophobic $-\text{SiCPh}_2$ groups had been incorporated successfully into its silicate network.³ These findings elucidated that the silicate compositions of catalyst **5** was the inorganosilicate networks of $(\text{OH})\text{Si}(\text{OSi})_3$ and $\text{Si}(\text{OSi})_4$ with the organosilicate $\text{R}-\text{Si}(\text{OSi})_3$ and $-\text{SiCPh}_2$ groups as its main part of silica walls.^{3, 10}

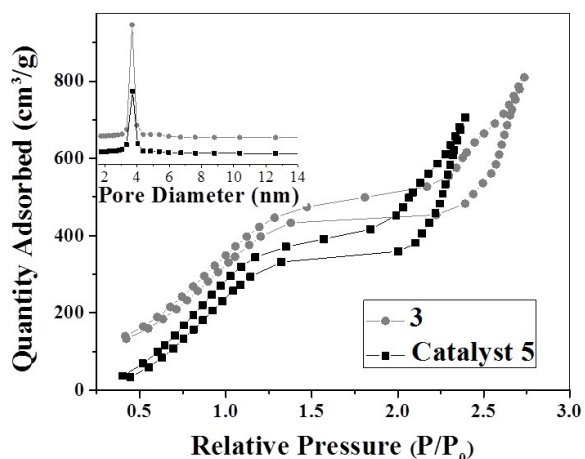


Fig. 3 Nitrogen adsorption-desorption isotherms of **3** and catalyst **5**.

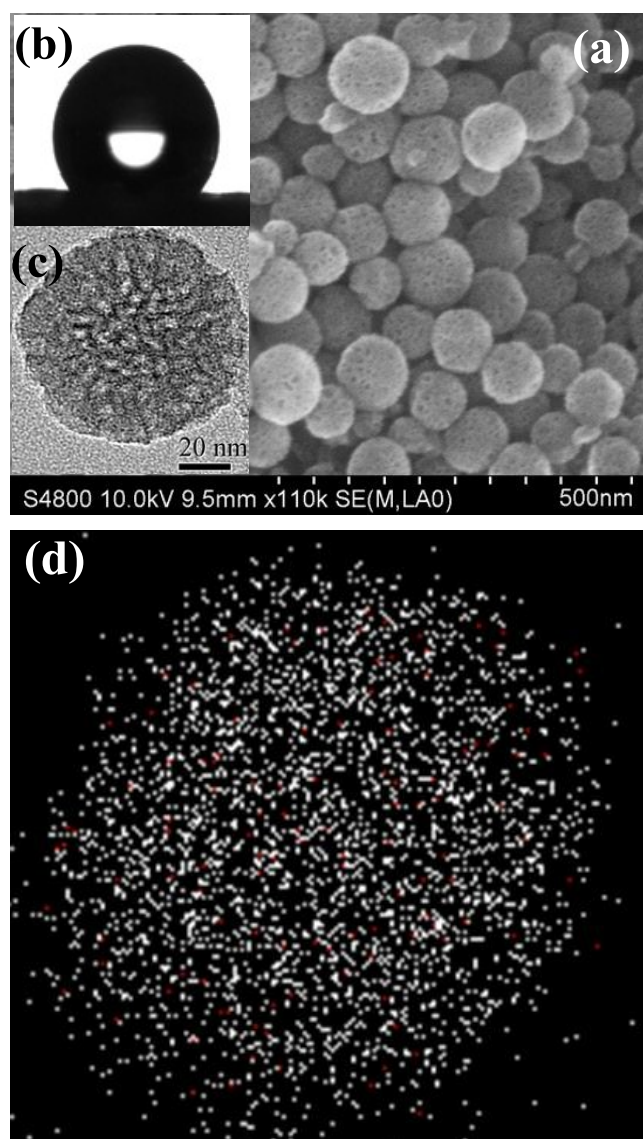


Fig. 4 (a) SEM image of **5**, (b) TEM image of **5**, (c) the water contact angle of **5**, and (d) SEM image with a chemical mapping of **5** showing the distribution of Si (white) and Ru (red).

In order to demonstrate the morphology, pore structure and rhodium distribution of catalyst **5**, its nitrogen adsorption-desorption isotherms, scanning electron microscopy (SEM), and transmission electron microscopy (TEM) images were further investigated. As shown in Figure 3, the nitrogen adsorption-desorption isotherms exhibited that both **3** and catalyst **5** were mesoporous due to the presence of typical IV characters with an H_1 hysteresis loop, which are the similar to the corresponding pure material.³ As compared their structural parameters, the catalyst **5** relative to its parent material **3** had a decrease in the mesopore size (3.66 nm versus 3.69 nm), surface area (443.2 cm²/g versus 462.1 cm²/g), and pore volume (0.49 cm³/g versus 0.51 cm³/g), suggesting the complexation of **3** with (Cp**RhCl*₂)₂ made the nanopore of catalyst **5** narrow. As shown in Figure 4, the SEM image revealed that catalyst **5** was composed of the uniformly dispersed nanoparticles with an average size of about 80 nm (Figure 4a), where its water contact angle was 130 °C (Figure 4b). The TEM image (Figure 4c) further confirmed its mesostructure, where the TEM image with a chemical mapping technique disclosed that the rhodium centers were uniformly distributed within its silicate network (Figure 4d).

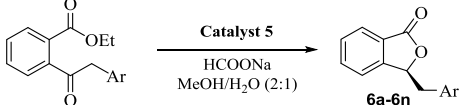
All these structural analyses and characterizations expatiate that a hydrophobic heterogeneous catalyst could be constructed steadily through the incorporation of chiral rhodium/diamine active center with the silicate network, where the well-defined single-site chiral rhodium/diamine-functionality verified by the ¹³C CP/MAS NMR spectrum, the hydrophobic nature proved by the water contact angle, uniformly dispersed nanoparticles confirmed by the SEM image, and highly dispersive active centers indicated at a TEM mapping, would govern its efficiently catalytic performance discussed below.

3.2. Catalytic performance of the heterogeneous catalysts

Chiral N-sulfonylated diamine-based (TsDPEN-based) organometallic complexes, as a kind of efficient asymmetric transfer hydrogenation (ATH) catalysts, had been applied extensively in various enantioselective reactions.^{8, 11} With the heterogeneous catalyst **5** in hand, we chose enantioselective tandem reduction/lactonization of ethyl 2-acrylylcarboxylates as a model reaction to test its catalytic performance.¹² According to the reported method,^{12a} the reduction/lactonization of ethyl 2-(2-phenylacetyl)benzoate was carried out through the use of 1.0 mol% of **5** as a catalyst and the HCOONa as a hydrogen source. It was found that this enantioselective reaction could afford the chiral products of (*S*)-3-benzylisobenzofuran-1(3*H*)-one in 99% yield and 99% *ee*, which was better than that of its homogeneous counterpart, Cp**RhTsDPEN*^{12a} (Entry 1 vs Entry 2, Table 1). Notably, such a high level of enantioselectivity was attributed to the well-defined single-site chiral rhodium/diamine species in **5** confirmed by its ¹³C CP/MAS NMR. This judgement could be further proved by a comparison of their XPS investigations. It was found that both catalyst **5** and its homogeneous Cp**RhTsDPEN* had the similar Rh 3d^{5/2} electron binding energy (309.2 eV versus 309.3 eV) (see Fig. S2 of ESI), further confirming that the well-defined single-site Cp**RhArDPEN*-functionality within its silicate network was responsible for the highly enantioselective performance.

On the basis of the above efficient catalytic performance in the enantioselective tandem reduction/lactonization of ethyl 2-(2-phenylacetyl)benzoate, a series of aryl-substituted substrates were further investigated under the same reaction conditions for the general applicability of catalyst **5**. As shown in Table 1, it was found that all the tested substrates could be converted into the corresponding chiral phthalides in high yields with excellent enantioselectivities under the same reaction conditions. It was noteworthy that the structural and electronic properties of substituents at the aromatic ring did not affect significantly their enantioselectivities, where the reactions with various electron-withdrawing and electron-donating substituents at the aromatic ring were equally efficient (Entries 4–14). In addition, the other substrates, such as ethyl 2-(2-(naphthalen-1-yl)acetyl)benzoate and ethyl 2-(2-(naphthalen-2-yl)acetyl)benzoate could also be converted into the corresponding chiral phthalides with excellent enantioselectivities (Entries 15–16).

Table 1. The enantioselective tandem reduction/lactonization of ethyl 2-acylarylcarboxylates.^a



Entry	Ar (6)	Time (h)	% Yield	% ee ^b
1	Ph (6a)	5	99	99
2	Ph (6a)	10	97	96 ^c
3	Ph (6a)	10	45	83 ^d
4	4-FPh (6b)	5	97	99
5	2,4-F ₂ C ₆ H ₃ (6c)	5	94	98
6	4-ClPh (6d)	5	96	94
7	2-ClPh (6e)	5	91	99
8	4-BrPh (6f)	5	93	99
9	4-CF ₃ Ph (6g)	5	95	99
10	3-CF ₃ Ph (6h)	5	96	98
11	4-MePh (6i)	5	93	98
12	4-OMePh (6j)	5	92	99
13	3-OMePh (6k)	5	93	99
14	3,4-(MeO) ₂ C ₆ H ₃ (6l)	5	91	98
15	1-naphthyl (6m)	5	93	98
16	2-naphthyl (6n)	5	93	99

^a Reaction conditions: catalyst **5** (21.65 mg, 2.0 μmol of Rh based on the ICP analysis), HCO₂Na (1.0 mmol), 2-acylarylcarboxylates (0.20 mmol), and 3.0 mL MeOH/H₂O (2:1), reaction temperature (40 °C). ^b Determined by chiral HPLC analysis (see Fig. S7 and S11 of ESI). ^c Data were obtained using homogeneous Cp*RhTsDPEN as a catalyst. ^d Data were obtained using its analogue **5'** as a catalyst.

To gain insight into the hydrophobic nature of catalyst **5** and to investigate the factors affecting catalytic performance, a comparable SiO₂-based Cp*RhArDPEN-functionalized inorganosilicate analogue **5'** as a parallel catalyst was also synthesized. In this case, **5'** was prepared by a two-component condensation of tetraethoxysilane and **1** following the similar

procedure (see experiment part of ESI and Figure S6). Only difference from the catalyst **5** is that **5'** is an inorganosilicate analogue and its inorganosilicate network has not the hydrophobic -SiCPh₂ groups. Taking use of this analogue **5'** as a parallel catalyst, we compared its catalytic performance in the enantioselective tandem reduction/lactonization of ethyl 2-(2-phenylacetyl)benzoate. The result showed that the reaction catalyzed by its analogue **5'** within 10 h only afforded the corresponding chiral products in 45% yield with 83% ee (Entry 3). This finding suggested that the absence of hydrophobic -SiCPh₂ groups in its silicate network of **5'** led to a poor catalytic performance, indicating the hydrophobic benefit of the designed catalyst **5**. A direct evidence supports this judgment coming from a kinetic investigation in the enantioselective reaction of ethyl 2-(2-phenylacetyl)benzoate. As shown in Figure 5, it was found that the reaction catalysed by **5** resulted in initial activity higher than that of its homogeneous Cp*RhTsDPEN, and markedly better than that attained with **5'** (the initial TOFs within 1 h were 73, 48 and 13 molmol⁻¹h⁻¹, respectively), further confirming the benefit the hydrophobic advantage of **5**.

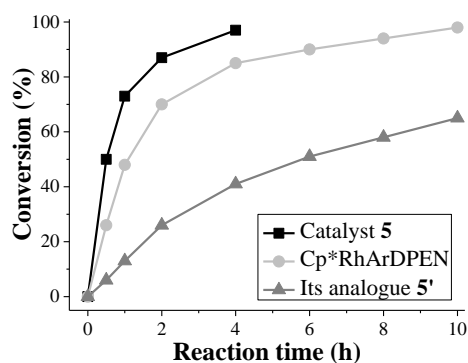
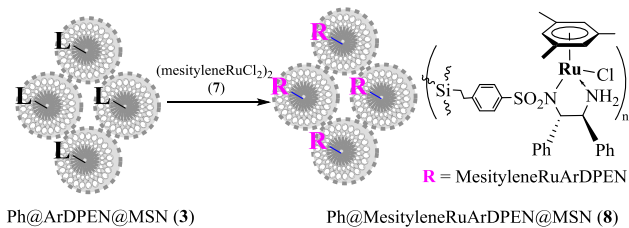


Fig. 5 Comparison of the enantioselective reaction of ethyl 2-(2-phenylacetyl)benzoate catalyzed by catalyst **5**, its homogeneous Cp*RhTsDPEN and its analogue **5'** (Reactions were carried out using 1.0 mol% of the catalyst at 40 °C).



Scheme 2. Preparation of heterogeneous catalyst **8**.

It was worth mentioning that the super-hydrophobic mesostructured silica as a chiral organometallics immobilization platform could be used to construct the other hydrophobic heterogeneous catalysts for enantioselective reaction. As shown in Scheme 2, the hydrophobic chiral ruthenium/diamine-functionalized mesostructured nanoparticles, abbreviated as Ph@MesityleneRuArDPEN@MSNs (**8**) (MesityleneRuArDPEN:¹¹ mesitylene = 1,3,5-trimethylbenzene,

where ArDPEN = ((S,S)-4-((trimethoxysilyl)ethyl)phenylsulfonyl-1,2-diphenylethylene-diamine), was also prepared from Ph@ArDPEN@MSNs (**3**) via a similar procedure. In this case, direct complexation of **3** with (mesityleneRhCl₂)₂ (**7**), followed by a Soxhlet extraction, afforded catalyst **8** as a light-yellow powder (see Fig. S1, S3–S6 of ESI).

Table 2. The DKR–ATH of α -benzoyl- β -ketophosphonates.^a

Entry	Ar (9)	%Yield	% <i>ee</i> ^b	<i>dr</i>
1	Ph (9a)	99	99	99:1
2	Ph (9a)	98	99	99:1 ^c
3	4-FPh (9b)	94	93	99:1
4	4-ClPh (9c)	96	96	99:1
5	4-ClPh (9d)	95	96	99:1
6	4-CNPh (9e)	93	95	99:1
7	4-CO ₂ Me (9f)	92	99	99:1
8	4-MePh (9g)	96	98	99:1
9	3-MePh (9h)	95	98	99:1
10	4-OMePh (9i)	94	95	99:1
11	2-naphthyl (9j)	91	99	99:1
12	2-thienyl (9k)	93	99	99:1

^a Reaction conditions: catalyst **8** (12.75 mg, 0.50 μ mol of Ru based on ICP analysis), α -benzoyl- β -ketophosphonates (0.10 mmol), 0.10 mL of HCOOH–Et₃N (5:2), and 3.0 mL of CH₂Cl₂, reaction temperature (35 $^{\circ}$ C), reaction time (24–30 h). ^b Determined by chiral HPLC analysis (see Fig. S8 and S11 of ESI). ^c Data were obtained using homogeneous MesityleneRuTsDPEN as a catalyst.

Having obtained catalyst **8**, we then explored a challenging dynamic kinetic resolution by asymmetric transfer hydrogenation (a DKR–ATH method¹³) for construction of 1,2-distereocentered diethyl α -benzoyl- β -hydroxyphosphonates¹⁴ based on those well-established DKR–ATH process in preparations of various 1,2-distereocentered α -substituted β -hydroxy ketones/esters/amides.¹⁵ In this case, we investigated the **8**-catalysed DKR–ATH process using the dynamic reduction of diethyl (2-(benzyloxy)-3-oxo-3-phenylpropanoyl)phosphonate as a model substrate. The reaction was carried out with 0.5 mmol% of **8** as a catalyst and the azeotropic mixture of HCO₂H–NEt₃ (5:2) as a hydrogen source. The result showed that chiral products of diethyl (R,R)-(2-(benzyloxy)-3-hydroxy-3-phenylpropanoyl)phosphonite in 99% yield with high levels of stereoselectivity (99:1 *dr* and 99% *ee*) could be obtained, which was comparable to that attained with its homogeneous counterpart, MesityleneRuTsDPEN¹⁴ (Entry 1 vs Entry 2, Table 2). Similarly, a series of aryl-substituted substrates could be converted into the corresponding chiral products in high yields with high levels of stereoselectivity under the same reaction conditions, suggesting its general applicability.

Another important aim in the design of the heterogeneous catalysts **5** and **8** is the ease of separation by simple centrifugation,

and its ability to retain its catalytic activity and enantioselectivity after multiple recycles. As we expected, catalyst **5** and **8** could be recovered through high-speed centrifugation and recycled repeatedly. As shown in Figure 6, in eighth consecutive reactions, the recycled catalyst **5** still gave 90% yield and 98% *ee* in the enantioselective tandem reduction/lactonization of ethyl 2-(2-phenylacetyl)benzoate (see Table S1 and Fig. S9 of ESI). Also, the recycled catalyst **8** could be used repeatedly for seven times in the DKR–ATH of diethyl (2-(benzyloxy)-3-oxo-3-phenylpropanoyl)phosphonite (see Table S2 and Fig. S10 of ESI).

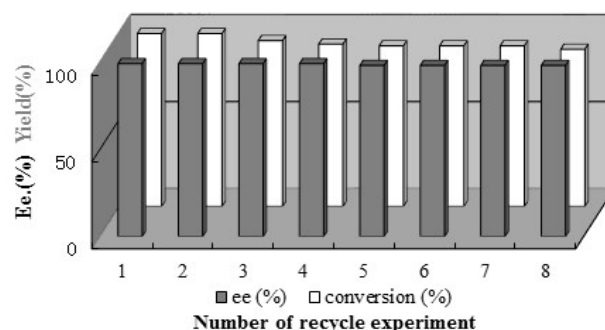


Fig. 6 Reusability of catalyst **5** in the entioselective tandem reduction/lactonization of ethyl 2-(2-phenylacetyl)benzoate as a substrate.

Conclusions

In conclusions, by utilizing a super-hydrophobic mesostructured silica, we develop two rhodium/diamine- and ruthenium/diamine-functionalized heterogeneous catalysts through the combination of chiral organometallic complexes within its silicate networks. As demonstrated in the present study, both heterogeneous catalysts exhibit excellent catalytic and enantioselective performance in two types of asymmetric reactions, where chiral rhodium/diamine-functionalized catalyst promotes greatly the enantioselective tandem reduction/lactonization of ethyl 2-acylarylcarboxylates to various chiral phthalides and chiral ruthenium/diamine-functionalized catalyst boosts an efficient asymmetric transfer hydrogenation–dynamic kinetic resolution process for construction of 1,2-distereocentered diethyl α -benzoyl- β -hydroxyphosphonates. As designed, the combined multifunctionalities of high hydrophobicity, and well-defined single-site active catalytic nature and uniformly distributed nanoparticles contribute cooperatively the highly catalytic performance. Furthermore, the heterogeneous catalysts could be recovered conveniently and reused repeatedly. The study described here highlights hydrophobic heterogeneous catalysts realize highly efficient asymmetric reactions.

Acknowledgements

We are grateful to China National Natural Science Foundation (21672149), and Ministry of Education of China (PCSIRT-IRT-16R49) for financial support.

References

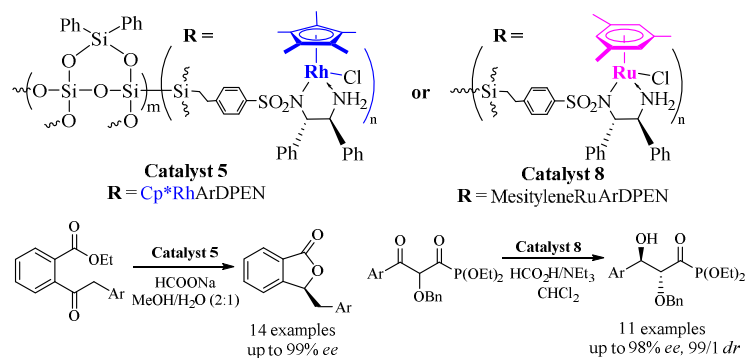
- (a) F. Kleitz, In *Handbook of Asymmetric Heterogeneous Catalysis*. Wiley–VCH, Weinheim, 2008, pp 25–72; (b) D. E. De Vos, M. Dams, B. F. Sels, P. A. Jacobs, *Chem. Rev.*, 2002, **102**, 3615–3640; (c) S.

- Minakata, M. Komatsu, *Chem. Rev.*, 2009, **109**, 711–724; (d) M. Bartók, *Chem. Rev.*, 2010, **110**, 1663–1705; (e) A. Mehdi, C. Reye, R. Corriu, *Chem. Soc. Rev.*, 2011, **40**, 563–574; (f) H. Q. Yang, L. Zhang, L. Zhong, Q. H. Yang, C. Li, *Angew. Chem. Int. Ed.*, 2007, **46**, 6861–6865.
- 5 2. (a) M. Thomas, J. R. Raja, *Acc. Chem. Res.*, 2008, **41**, 708–720; (b) Yu, C. G. He, J. *Chem. Commun.*, 2012, **48**, 4933–4940; (c) C. Li, H. D. Zhang, D. M. Jiang, Q. H. Yang, *Chem. Commun.*, 2007, 547–558.
3. J. Peng, Y. Yao, X. M. Zhang, C. Li, Q. H. Yang, *Chem. Commun.*, 2014, **50**, 10830–10833.
- 10 4. (a) K. S. Liu, X. Yao, L. Jiang, *Chem. Soc. Rev.*, 2010, **39**, 3240–3255; (b) M. A. Cambor, A. Corma, P. Esteve, A. Martínez, S. Valencia, *Chem. Commun.*, 1997, 795–796; (c) A. Corma, M. Domine, J. A. Gaona, J. L. Jordá, M. T. Navarro, F. Rey, J. Pérez-Pariente, J. P. Tsuji, B. McCulloch, L. T. Nemeth, *Chem. Commun.*, 1998, 2211–2212; (d)
- 15 T. Blasco, M. A. Cambor, A. Corma, P. Esteve, J. M. Guil, A. Martínez, J. A. Perdigón-Melón, S. Valencia, *J. Phys. Chem. B.*, 1998, **102**, 75–88; (e) H. Shintaku, K. Nakajima, M. Kitano, M. Hara, *Chem. Commun.*, 2014, **50**, 13473–13476; (f) J. Xiong, W. S. Zhu, W. J. Ding, L. Yang, M. Zhang, W. Jiang, Z. Zhao, H. M. Li, *RSC Adv.*, 2015, **5**, 16847–16855; (g) H. Q. Yang, X. Jiao, S. R. Li, *Chem. Commun.*, 2012, **48**, 11217–11219.
5. (a) K. Zhang, L. L. Xu, J. G. Jiang, N. Calin, K. F. Lam, S. J. Zhang, H. H. Wu, G. D. Wu, B. Albel, L. Bonneviot, P. Wu, *J. Am. Chem. Soc.*, 2013, **135**, 2427–2430; (b) F. Q. Tang, L. L. Li, D. Chen, *Adv. Mater.*, 2012, **24**, 1504–1534; (c) Z. A. Qiao, L. Zhang, M. Y. Guo, Y. L. Liu, Q. S. Huo, *Chem. Mater.*, 2009, **21**, 3823–3829; (d) W. C. Yoo, A. Stein, *Chem. Mater.*, 2011, **23**, 1761–1767; (e) Z. Gao, I. Zharov, *Chem. Mater.*, 2014, **26**, 2030–2037; (f) M. H. Wang, Z. K. Sun, Q. Yue, J. Yang, X. Q. Wang, Y. H. Deng, C. Z. Yu, D. Y. Zhao, *J. Am. Chem. Soc.*, 2014, **136**, 1884–1892; (g) Y. Ma, L. Xing, H. Zheng, S. Che, *Langmuir*, 2011, **27**, 517–520; (h) D. S. Moon, J. K. Lee, *Langmuir*, 2012, **28**, 12341–12347; (i) M. J. Stébé, M. Emo, A. F. L. Follovec, L. Metlas-Komunjer, I. Pezron, J. L. Blin, *Langmuir*, 2013, **29**, 1618–1626.
- 35 6. (a) C. Chen, J. Xu, Q. H. Zhang, Y. F. Ma, L. P. Zhou, M. Wang, *Chem. Commun.*, 2011, **47**, 1336–1338; (b) S. Shi, M. Wang, C. Chen, J. Gao, H. Ma, J. P. Ma, J. Xu, *Chem. Commun.*, 2013, **49**, 9591–9593; (c) M. Wang, F. Wang, J. P. Ma, C. Chen, S. Shi, J. Xu, *Chem. Commun.*, 2013, **49**, 6623–6625.
- 40 7. (a) H. S. Zhang, R. H. Jin, H. Yao, S. Tang, J. L. Zhuang, G. H. Liu, H. X. Li, *Chem. Commun.*, 2012, **48**, 7874–7876; (b) F. Gao, R. H. Jin, D. C. Zhang, Q. X. Liang, Q. Q. Ye, G. H. Liu, *Green Chem.*, 2013, **15**, 2208–2214; (c) J. Y. Wang, L. Wu, X. Y. Hu, R. Liu, R. H. Jin, G. H. Liu, *Catal. Sci. Technol.*, 2017, **7**, 4444–4450; (d) J. Z. An, T. Y. Cheng, X. Xiong, L. Wu, B. Han, G. H. Liu, *Catal. Sci. Technol.*, 2016, **6**, 5714–5720; (e) M. Wu, L. Y. Kong, K. W. Wang, R. H. Jin, T. Y. Cheng, G. H. Liu, *Catal. Sci. Technol.*, 2015, **5**, 1750–1757. (f) R. Liu, T. Y. Cheng, L. Y. Kong, C. Chen, G. H. Liu, H. X. Li, *J. Catal.*, 2013, **307**, 55–61.
8. (a) T. Ikariya, A. J. Blacker, *Acc. Chem. Res.*, 2007, **40**, 1300–1308; (b)
- 50 J. E. D. Martins, G. J. Clarkson, M. Wills, *Org. Lett.*, 2009, **11**, 847–850; (c) R. Malacea, R. Poli, E. Manoury, *Coord. Chem. Rev.*, 2010, **254**, 729–752.
9. J. Mao, D. C. Baker, *Org. Lett.*, 1999, **1**, 841–843.
10. O. Kröcher, O. A. Köppel, M. Fröba, A. Baiker, *J. Catal.*, 1998, **178**, 284–298.
- 55 11. (a) S. Hashiguchi, A. Fujii, J. Takehara, T. Ikariya, R. Noyori, *J. Am. Chem. Soc.*, 1995, **117**, 7562–7563; (b) A. M. Hayes, D. J. Morris, G. J. Clarkson, M. Wills, *J. Am. Chem. Soc.*, 2005, **127**, 7318–7319; (c) P. N. Liu, P. M. Gu, F. Wang, Y. Q. Tu, *Org. Lett.*, 2004, **6**, 169–172; (d) X. Wu, X. Li, W. Hems, F. King, J. Xiao, *Org. Biomol. Chem.*, 2004, **2**, 1818–1821; (e) A. Fujii, S. Hashiguchi, N. Uematsu, T. Ikariya, R. Noyori, *J. Am. Chem. Soc.*, 1996, **118**, 2521–2522; (f) T. Ikariya, A. J. Blacker, *Acc. Chem. Res.*, 2007, **40**, 1300–1308; (g) T. Ohkuma, K. Tsutsumi, N. Utsumi, N. Arai, R. Noyori, K. Murata, *Org. Lett.*, 2007, **9**, 255–257.
- 65 12. (a) B. Zhang, M. H. Xu, G. Q. Lin, *Org. Lett.*, 2009, **11**, 4712–4715; (b) D. H. T. Phan, B. Kim, V. M. Dong, *J. Am. Chem. Soc.*, 2009, **131**, 15608–15609; (c) S. K. Murphy, V. M. Dong, *J. Am. Chem. Soc.*, 2013, **135**, 5553–5556.
- 70 13. (a) K. M. Steward, M. T. Corbett, C. G. Goodman, J. S. Johnson, *J. Am. Chem. Soc.*, 2012, **134**, 20197–20206; (b) K. M. Steward, E. C. Gentry, J. S. Johnson, *J. Am. Chem. Soc.*, 2012, **134**, 7329–7332.
14. S. M. Son, H. K. Lee, *J. Org. Chem.*, 2014, **79**, 2666–2681.
15. (a) A. Ros, A. Magriz, H. Dietrich, J. M. Lassaletta, R. Fernández, *Tetrahedron*, 2007, **63**, 7532–7537; (b) F. Eustache, P. I. Dalko, J. Cossy, *Org. Lett.*, 2002, **4**, 1263–1265; (c) Y. Wu, Z. Geng, J. Bai,
- 75 16. Y. Zhang, *Chin. J. Chem.*, 2011, **29**, 1467–1472; (d) D. Cartigny, K. Püntener, T. Ayad, M. Scalone, V. Ratovelomanana-Vidal, *Org. Lett.*, 2010, **12**, 3788–3791; (e) Z. Liu, C. S. Shultz, C. A. Sherwood, S. Kraska, P. G. Dormer, R. Desmond, C. Lee, E. C. Sherer, J. Shpungin, J. Cuff, F. Xu, *Tetrahedron Lett.*, 2011, **52**, 1685–1688; (f) B. Seashore-Ludlow, F. Saint-Dizier, P. Somfai, *Org. Lett.*, 2012, **14**, 6334–6337; (g) B. Seashore-Ludlow, P. Villo, P. Somfai, *Chem. Eur. J.*, 2012, **18**, 7219–7223; (h) G. Kumaraswamy, A. Narayana Murthy, V. Narayanarao, S. P. B. Vemulapalli, J. Bharatam, *Org. Biomol. Chem.*, 2013, **11**, 6751–6765; (i) J. Limanto, S. W. Kraska, B. T. Dorner, E. Vazquez, N. Yoshikawa, L. Tan, *Org. Lett.*, 2010, **12**, 512–515; (j) S. M. Son, H. K. Lee, *J. Org. Chem.*, 2013, **78**, 8396–8404.

Graphical Abstract :

A super-hydrophobic mesostructured silica as a chiral organometallics immobilization platform for heterogeneous asymmetric catalysis

Bing Han, Lei Zhao, Yongkang Song, Zhongrui Zhao, Dongfeng Yang, Rui Liu* and Guohua Liu*



Super-hydrophobic mesostructured silica-supported molecule catalysts are developed and their applications in enantioselective organic transformation are investigated.